A Stochastic Model of Bipolar Resistive Switching in Metal-Oxide-Based Memory

Alexander Makarov, Viktor Sverdlov, and Siegfried Selberherr
Institute for Microelectronics, TU Wien
Vienna, Austria
Email: {makarov | sverdlov | selberherr}@iue.tuwien.ac.at

***Abstract* — A stochastic model of the resistive switching mechanism in bipolar metal-oxide-based resistive random access memory (RRAM) is presented. The distribution of electron occupation probabilities obtained is in agreement with previous work. In particular, a low occupation region is formed near the cathode. Our simulations of the temperature dependence of the electron occupation probability near the anode and the cathode demonstrate a high robustness of the low occupation region. This result indicates that a decrease of the switching time with increasing temperature cannot be explained only by reduced occupations of the vacancies in the low occupation region, but is related to an increase of the mobility of the oxide ions. A hysteresis cycle of a RRAM simulated with our stochastic model is in good agreement with experimental results.**

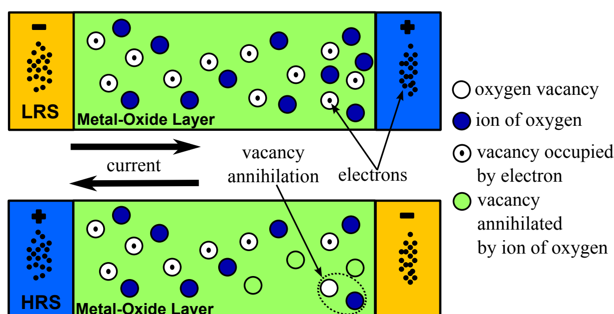

Figure 1. Schematic illustration of the conducting filament in the low resistance state (top) and the high resistance state (bottom).

I. INTRODUCTION

With flash memories rapidly approaching the physical limits of scalability, research on new nonvolatile memory concepts has significantly accelerated. Several new memory concepts as potential substitutes of the flash memory were invented and developed: a technology of phase change RAM (PCRAM), spin transfer torque RAM (STTRAM), carbon nanotube RAM (NRAM), copper bridge RAM (CBRAM), racetrack memory, and resistive RAM (RRAM). A new type of nonvolatile memory must exhibit low operating voltages, low power consumption, high operation speed, long retention time, high endurance, simple structure, and small size [1].

One of the most promising candidates for future universal memory is the resistive random access memory (RRAM). It is based on new materials, such as metal oxides [2-4] and perovskite oxides [5]. This type of memory is characterized by high density, excellent scalability, low operating voltages (<2V), fast switching times (<10ns), and long retention time.

In the literature a broad spectrum of electronic and/or ionic switching mechanisms for oxide-based memory has been suggested: a model based on trapping of charge carriers [6], electrochemical migration of oxygen vacancies [7, 8], electrochemical migration of oxygen ions [9, 10], a unified physical model [11, 12], a domain model [13], a filament anodization model [14], a thermal dissolution model [15], and others. Unfortunately, a proper fundamental understanding of the switching mechanism is still missing.

In this work we present a stochastic model of the bipolar resistive switching mechanism based on electron hopping between the oxygen vacancies along the conductive filament in an oxide layer.

II. MODEL DESCRIPTION

We associate the resistive switching behavior in oxide-based memory with the formation and rupture of a conductive filament (CF). The CF is formed by localized oxygen vacancies (V_o) [11, 12] or domains of V_o (Fig. 1). Formation and rupture of a CF is due to a redox reaction in the oxide layer under a voltage bias. The conduction is due to electron hopping between these V_o.

For modeling the resistive switching in bipolar oxide-based memory by Monte Carlo techniques, we describe the dynamics of oxygen ions (O^{2-}) and electrons in an oxide layer as follows:

This research is supported by the European Research Council through the grant #247056 MOSILSPIN.

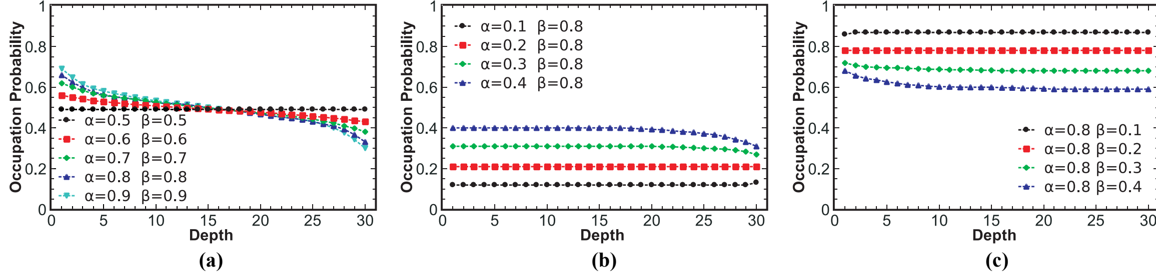

Figure 2. Calculated distribution of electron occupation probabilities for unidirectional next nearest neighbor hopping between the V_o (the 1st V_o is near the cathode, the last V_o is near the anode): (a) α>0.5 and β>0.5, p_c=0.5; (b) α<0.5 and α<β, p_c=α; (c) β<0.5 and β<α, p_c=1-β.

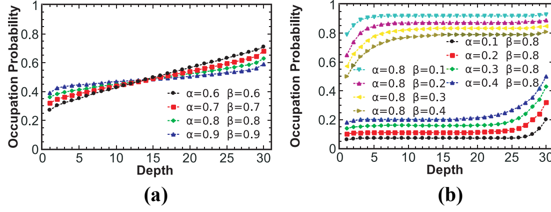

Figure 3. Calculated distribution of electron occupation probabilities, if unidirectional hopping is allowed not only to/from the closest V_o: (a) α>0.5 and β>0.5; (b) α<0.5 and α<β; β<0.5 and β<α.

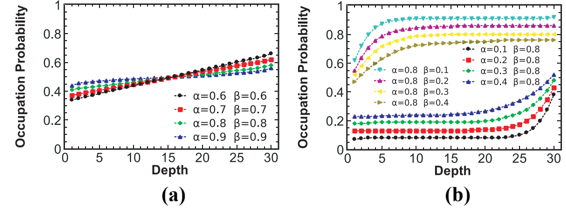

Figure 4. Calculated distribution of electron occupation probabilities, for hopping according to (1-3), for T>0: (a) α>0.5 and β>0.5; (b) α<0.5 and α<β; β<0.5 and β<α.

- formation of V_o by O^{2-} moving to an interstitial position;
- annihilation of V_o by moving O^{2-} to V_o;
- an electron hop into V_o from an electrode;
- an electron hop from V_o to an electrode;
- an electron hop between two V_o.

In order to model the dependences of transport on the applied voltage and temperature we choose the hopping rates for electrons as [16]:

$$\Gamma_{nm} = A_e \cdot \frac{dE}{1-\exp(-dE/T)} \cdot \exp(-R_{nm}/a) \quad (1)$$

Here, A_e is a coefficient, $dE=E_n-E_m$ is the difference between the energies of an electron positioned at sites n and m, R_{nm} is the hopping distance, a is the localization radius. The hopping rates between an electrode (*0* or *N+1*) and an oxygen vacancy m are described [12]:

$$\Gamma_m^{iC} = \alpha \cdot \Gamma_{0m}, \Gamma_m^{oC} = \alpha \cdot \Gamma_{m0} \quad (2)$$

$$\Gamma_m^{iA} = \beta \cdot \Gamma_{(N+1)m}, \Gamma_m^{oA} = \beta \cdot \Gamma_{m(N+1)} \quad (3)$$

Here, α and β are the coefficients of the boundary conditions on the cathode and anode, respectively, N is the number of sites, A and C stand for cathode and anode, and i and o for hopping on the site and out from the site, respectively.

The current generated by hopping is calculated as:

$$I = q_e \cdot \sum dx / \sum \left(1 / \sum_m \Gamma_m \right) \quad (4)$$

III. Model Verification

All calculations are made on one or/and two-dimensional lattices, the distances between two nearest neighboring V_o in all directions are equal. All V_o are at the same energy level, if no voltage or temperature is applied. Despite the fact that in the binary metal oxides, oxygen vacancies can have three different charge states with charge 0, +1, +2, to simplify the calculations, we assume that the oxygen vacancy is either empty or occupied by one electron.

A. Calculation of electron ocupation probability

To verify the proposed model, we first evaluate the average electron occupations of hopping sites under different conditions. For comparison with previous works all calculations in this subsection are made on a one-dimension lattice consisting of thirty equivalent, equidistantly positioned hopping sites V_o.

Following [17], we first allow hopping in one direction and only to/from the closest V_o. The occupation probability of central oxygen vacancies, p_c, is described, depending on the boundary conditions as follows: 1) for α>0.5 and β>0.5, p_c=0.5; 2) for α<0.5 and α<β, p_c=α; 3) for β<0.5 and β<α, p_c=1-β. Fig.2 shows simulation results of our stochastic model, which are fully consistent with theoretical predictions [17].

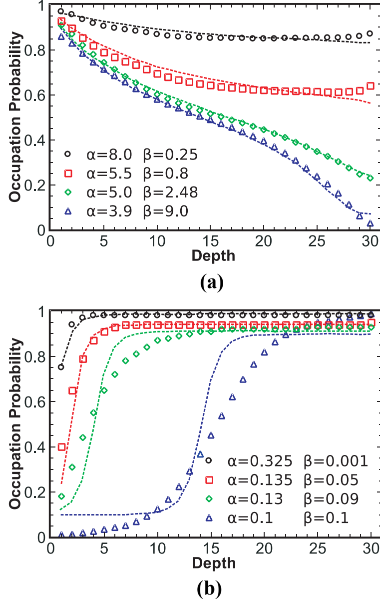

Figure 5. Calculated distribution of electron occupation probabilities under different biasing voltages. Lines are from [12], symbols are obtained from our stochastic model.

To move from a model system [17] to a more realistic structure, we calculated the distribution of electron occupations for a chain, where hopping is allowed not only to/from the nearest V_o (Fig. 3), and for systems, where hopping (1-3) is allowed in both directions (Fig. 4). Note that for α>0.5 and β>0.5 (Fig. 3a and Fig. 4a) we still have p_c=0.5 in the center, while for other values α, β we observe a decrease in p_c for α<β and an increase in p_c for β<α.

We have calibrated our model in a manner to reproduce the results reported in [12], for V=0.4 V to V=1.6 V. Fig. 5a shows a case, when the hopping rate between the electrodes and V_o is larger than the rate between two V_o (i.e. α, β > 1). In this case the low occupation region is formed near the anode (unipolar behavior).

Fig. 5b shows a case, where the hopping rate between two V_o is larger than the rate between the electrodes and V_o (i.e. α, β < 1). In this case a low occupation region is formed near the cathode (bipolar behavior).

Note that when V=0 V, the probability of occupation of all vacancies becomes equal to 0.5 regardless of the voltage applied before. This result indicates that, after the voltage is turned off, the probability of a CF rupture should increase substantially due to a decrease of the occupation probability of the vacancies from 1 to 0.5. But in practice we do not observe this, so to associate a CF rupture only with the formation of the low occupation region is wrong.

B. *Modeling of temperature dependence*

With the model calibrated to [12] we simulated the temperature dependence of the site occupations in the low occupation region. The results shown in Fig. 6a and Fig. 6b indicate high robustness of the low occupation region demonstrating changes of less than 10%, when the temperature is elevated from 25° C to 200° C. At the same time this result indicates that the measured decrease of switching time with increasing temperature reported in [12] stems from the increased mobility of oxide ions, rather than from reduced occupations of V_o in the low occupation region.

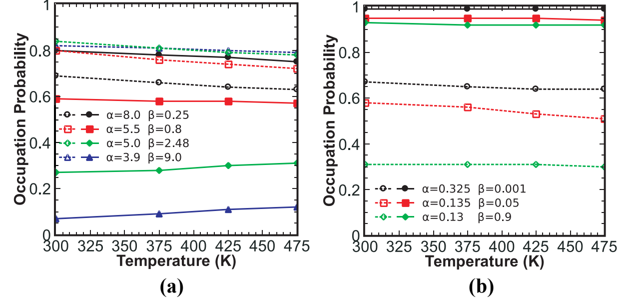

Figure 6. Temperature dependence of electron occupation probability near the anode (filled symbols) and the cathode (open symbols).

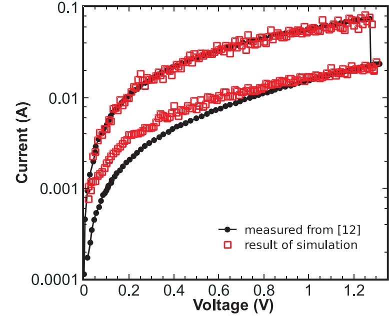

Figure 7. Current-voltage curves during reset process. Lines are measured result from [12], symbols are obtained from our stochastic model.

C. *Modeling of the RESET process*

Results obtained from simulations of the temperature dependence of the site occupations in the low occupation region demonstrate a necessity to include the dynamics of oxygen ions.

To describe the motion of ions we have chosen the ion rates similar to (1):

$$\Gamma_n^{'} = A_i \cdot \frac{dE}{1-\exp(-dE/T)} \tag{5}$$

Here we assume that O^{2-} can only move to the nearest interstitial. A distance-dependent term is thus included in A_i. dE includes the formation energy for the m-th V_o /annihilation energy of the m-th V_o, when O^{2-} is moving to an interstitial or back to V_o, respectively.

To verify the model, we simulated the reset I-V characteristics for a single-CF device [12]. For the simulations we have used a one-dimensional lattice consisting of thirty equivalent, equidistantly positioned hopping sites V_o. Near each V_o an oxygen ion is placed. Fig.7. shows the simulation results of the stochastic model, which are in perfect agreement with measurements from [12].

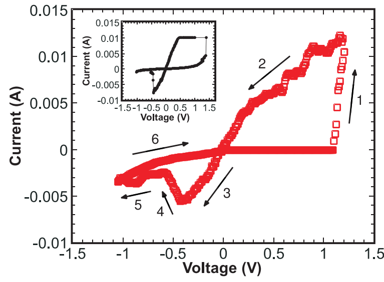

Figure 8. *I-V* characteristics showing the hysteresis cycle obtained from our stochastic model (α=0.1 and β=0.1). The inset shows the hysteresis cycle for *M*-ZnO-*M* from [4].

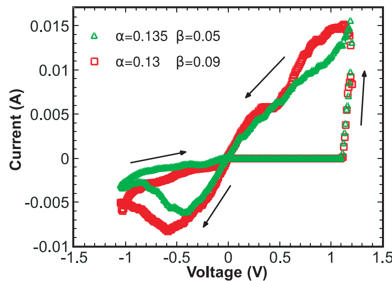

Figure 9. *I-V* characteristics showing hysteresis cycles obtained from the stochastic model for different parameters.

D. *Modeling of the hysteresis cycle*

All calculations of RRAM *I-V* characteristics are now performed on a two-dimensional lattice (2×30). We have investigated the *I-V* hysteresis by applying a saw-tooth like voltage V. We have assumed that the coefficients of the boundary conditions are constant and equal to 0.1. The simulated RRAM switching hysteresis cycle is shown in Fig.8. The cycle is in good agreement with the experimental one from [4] shown in the inset of Fig.8.

The interpretation of the RRAM hysteresis cycle obtained from the stochastic model is as follows. If a positive voltage is applied, the formation of a CF begins, when the voltage reaches a critical value sufficient to create V_o by moving O^{2-} to an interstitial position. This leads to a sharp increase in the current (Fig. 8 Segment 1) signifying a transition to a state with low resistance. When a reverse negative voltage is applied, the current increases linearly (Fig. 8 Segment 3), until the applied voltage reaches the value at which annihilation of V_o is triggered by means of moving O^{2-} to V_o. The CF is ruptured and so the current decreases (Fig. 8 Segment 4). This is the transition to a state with high resistance.

Interestingly, for parameters different from those in Fig.8 (α=0.135, β=0.05 and α=0.13, β=0.09) we still see a hysteresis cycle (Fig. 9), although the region of low occupation which, according to [12], is responsible for the rupture of the CF is almost absent. This result supports the observation that the ion dynamics is critical in describing the RRAM switching mechanism.

IV. CONCLUSION

In this work we have presented a stochastic model of the bipolar resistive switching mechanism. The distribution of the electron occupation probabilities calculated with the model is in excellent agreement with previous work. The simulated RRAM switching hysteresis cycle is in good agreement with the experimental result. We have shown that the process of rupture of the CF is determined by the dynamics of oxygen ions and not only by the formation of the low occupation region. The proposed stochastic model can be used for performance optimization of RRAM devices.

REFERENCES

[1] M. H. Kryder, C. S. Kim, "After Hard Drives - What Comes Next?," IEEE Trans. Magn., vol. 45, no. 10, pp. 3406-3413, 2009.

[2] C. Kugeler, C. Nauenheim, M. Meier, A. Rudiger, R. Waser, "Fast Resistance Switching of TiO_2 and MSQ Thin Films for Non-Volatile Memory Applications (RRAM)," NVM Tech. Symp., p. 6, 2008.

[3] Y. S. Chen, T. Y. Wu, P. J. Tzeng, "Forming-free HfO_2 Bipolar RRAM Device with Improved Endurance and High Speed Operation," Symp. on VLSI Tech., pp. 37-38, 2009.

[4] S. Lee, H. Kim, D. J. Yun, S. W. Rhee, K. Yong, "Resistive Switching Characteristics of ZnO Thin Film Grown on Stainless Steel for Flexible Nonvolatile Memory Devices," APL, vol. 95, no. 26, pp. 262113/1-3, 2009.

[5] C. C. Lin, C. Y. Lin, M. H. Lin, "Voltage-Polarity-Independent and High-Speed Resistive Switching Properties of V-Doped SrZrO3 Thin Films," IEEE Trans. Electron Devices, vol. 54, no. 12, pp. 3146-3151, 2007.

[6] T. Fujii, M. Kawasaki, A. Sawa, H. Akoh, Y. Kawazoe, and Y. Tokura, "Hysteretic Current–Voltage Characteristics and Resistance Switching at an Epitaxial Oxide Schottky Junction SrRuO3/SrTi0.99Nb0.01O3," APL, vol. 86, no. 1, art. no. 012107, 2005.

[7] Y. B. Nian, J. Strozier, N. J. Wu, X. Chen, A. Ignatiev, "Evidence for an Oxygen Diffusion Model for the Electric Pulse Induced Resistance Change Effect in Transition-Metal Oxides," PRL, vol. 98, no. 14, pp. 146403/1-4, 2007.

[8] S. X. Wu, L. M. Xu, X. J Xing, "Reverse-Bias-Induced Bipolar Resistance Switching in Pt/TiO2/SrTi0.99Nb0.01O3/Pt Devices," APL, vol. 93, no. 4, pp. 043502/1-3, 2008.

[9] K. Szot, W. Speier, G. Bihlmayer and R. Waser, "Switching the Electrical Resistance of Individual Dislocations in Single-Crystalline SrTiO3," Nature Materials, vol. 5, pp. 312-320, 2006.

[10] Y. Nishi, J. R. Jameson, "Recent Progress in Resistance Change Memory," Dev. Res. Conf. 2008, pp. 271-274, 2008.

[11] N. Xu, B. Gao, L. F. Liu, B. Sun, X. Y. Liu, R. Q. Han, J. F. Kang, and B. Yu, "A Unified Physical Model of Switching Behavior in Oxide-Based RRAM," Symp. on VLSI Tech., pp. 100-101, 2008.

[12] B. Gao, B. Sun, H. Zhang, L. Liu, X. Liu, R. Han, J. Kang, B. Yu, "Unified Physical Model of Bipolar Oxide-Based Resistive Switching Memory," IEEE Electron Device Lett., vol. 30, no. 12, pp. 1326-1328, 2009.

[13] M. J. Rozenberg, I. H. Inoue, and M. J. Sanchez, "Nonvolatile Memory with Multilevel Switching: A Basic Model," PRL, vol. 92, no. 17, pp. 178302-1, 2004.

[14] K. Kinoshita, T. Tamura, H. Aso, H. Noshiro, C. Yoshida, M. Aoki, Y. Sugiyama, H. Tanaka, "New Model Proposed for Switching Mechanism of ReRAM," IEEE Non-Volatile Semicond. Memory Workshop 2006, pp. 84 – 85, 2006.

[15] U. Russo, D. Ielmini, C. Cagli, A.L. Lacaita, S. Spiga, C. Wiemer, M. Perego, and M. Fanciulli, "Conductive-Filament Switching Analysis and Self-Accelerated Thermal Dissolution Model for Reset in NiO-Based RRAM," IEDM Tech. Dig., pp. 775-778, 2007.

[16] V. Sverdlov, A. N. Korotkov, K. K. Likharev, "Shot-Noise Suppression at Two-Dimensional Hopping," PRB, vol.63, 081302, 2001.

[17] B. Derrida, "An Exactly Soluble Non-Equilibrium System: The Asymmetric Simple Exclusion Process," Phys. Rep., vol. 301, no. 1-3, pp. 65-83, 1998.